Chemistry & Biology, Vol. 9, 1141–1148, October, 2002, ©2002 Elsevier Science Ltd. All rights reserved. PII S1074-5521(02)00241-7

NikR Repressor: High-Affinity Nickel Binding to the C-Terminal Domain Regulates Binding to Operator DNA

Peter T. Chivers[2] and Robert T. Sauer[1]
Department of Biology
Massachusetts Institute of Technology
Cambridge, Massachusetts 02139

Summary

***E. coli* NikR repressor binds operator DNA in a nickel-dependent fashion. The pM affinity of NikR for nickel is mediated by its C-terminal 86 residues. Nickel binding induced additional secondary structure, decreased the compactness, and increased the stability of NikR. Tetramer formation by the C-terminal domain and intact NikR did not require nickel. High-affinity nickel binding decreased the NikR concentration needed to half maximally protect operator DNA from undetectable levels to 30 nM. The intracellular concentration of NikR in *E. coli* is high enough that saturation of the high-affinity nickel sites should lead to substantial occupancy of the *nik* operator. Nickel binding to a set of low-affinity NikR sites resulted in an additional large increase in operator affinity and substantially increased the size of the NikR footprint on the operator.**

Introduction

The acquisition of trace metals poses a dilemma for cells. Some amount of each trace metal is required for cell viability, but excess levels can potentially be toxic. In general, tightly regulated metal uptake and efflux systems control this balance. Nickel, which seems to be used by all organisms, is most often utilized by microbes for growth under anaerobic conditions [1, 2]. For example, *Escherichia coli* under anaerobic conditions need high concentrations of nickel, acquired primarily through the NikABCDE nickel permease, to support the activity of Ni/Fe-hydrogenase [3].

Transcription of the *E. coli nikABCDE* operon is negatively regulated by the NikR repressor protein when intracellular nickel levels are high [4, 5]. NikR, which has orthologs in many bacteria and archaea, contains an N-terminal domain of roughly 50 residues and a C-terminal region of approximately 85 residues [6]. The N-domain dimer of NikR binds operator DNA and is homologous to homodimeric proteins such as Arc, CopG, and other members of the ribbon-helix-helix family of transcription factors. These proteins recognize operator DNA using a two-stranded antiparallel β sheet [7, 8]. The C-terminal portion of NikR is also necessary for high-affinity DNA binding and contains a unique pattern of conserved residues that are potential nickel ligands. Previous work suggested that NikR contains two types of nickel binding sites with different affinities [4]. Occupancy of the low-affinity nickel sites appeared to be required for formation of a high-affinity complex between NikR and the *nik* operator site [4]; the role of the high-affinity nickel binding sites was not determined.

In this paper, we have characterized the biochemical and biophysical properties of the C-terminal domain of NikR and have also probed the role of nickel binding in determining the affinity of NikR for its operator DNA. The C-terminal domain was found to be stably folded, to form tetramers, and to bind nickel ions with an apparent affinity of 2 pM. Nickel binding to these high-affinity sites induced additional secondary structure in the C-terminal domain and increased the stability of this fragment; similar nickel binding effects were observed for full-length NikR. Nickel binding was not, however, required for tetramerization of either the C-domain or of intact NikR. Nickel binding to the high-affinity sites in the C-terminal domain of NikR increased the protein's apparent affinity for operator DNA binding from a value weaker than 1 μM to roughly 30 nM. The intracellular concentration of NikR in *E. coli* grown under anaerobic conditions was found to be approximately 200 nM, suggesting that saturation of the high-affinity nickel sites in these repressor molecules would lead to substantial occupancy of the *nik* operator site. Nickel binding to the low-affinity (30 μM) NikR sites resulted in an additional large increase in the affinity of NikR for operator DNA and an increase in the size of the NikR footprint. The implications of these findings for NikR-mediated regulation of intracellular nickel uptake are discussed below.

Results

C-Domain and Nickel Binding

A fragment corresponding to the C-terminal 86 residues of *E. coli* NikR (Gly48 to Asp133) was cloned, expressed, and purified by Ni-NTA and anion-exchange chromatography. We will refer to this fragment as the C-domain. In initial studies, we found that this domain only bound to the Ni-NTA column when nickel was added prior to chromatography. When excess nickel was not added, the C-domain stripped nickel ions from the Ni-NTA column during chromatography. This behavior, which was also observed during purification of full-length NikR [4], suggested that the determinants for high-affinity nickel binding are located within the C-domain.

The UV-visible spectrum of the purified C-domain, like that of full-length NikR, had additional peaks indicative of nickel binding (Figure 1A). Incubation of the C-domain with EDTA for several days resulted in a spectrum expected for the protein alone. Following removal of the EDTA by desalting, addition of one nickel molecule per protein subunit restored the original absorbance spectrum of the nickel-bound C-domain. Subtracting the nickel-free spectrum from the nickel-bound spectrum showed nickel-dependent absorbance peaks at 240–242, 260, and 302 nm (Figure 1B). Although the positions of the nickel-associated absorbance maxima were the

[1]Correspondence: bobsauer@mit.edu
[2]Present address: Department of Biochemistry and Molecular Biophysics, Washington University School of Medicine, St. Louis, Missouri 63110.

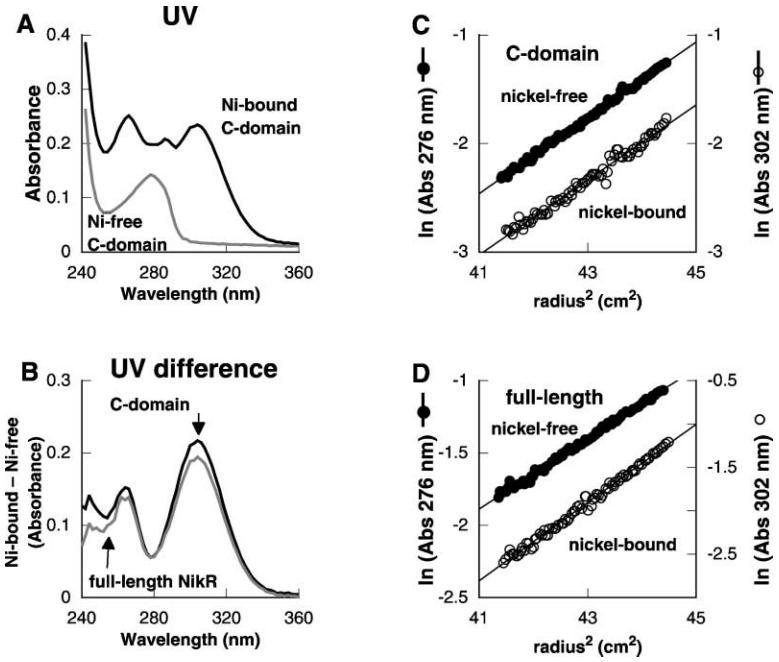

Figure 1. Nickel Binding and Oligomeric State

(A) UV-visible spectra of the nickel-bound and nickel-free forms of the NikR C-domain.

(B) Difference spectra of nickel-bound minus nickel-free forms of the C-domain or full-length NikR.

(C and D) Equilibrium sedimentation (20°C, 20 mM Tris [pH 7.5], 100 mM NaCl) of (C) 50 μM of nickel-free or nickel-bound C-domain and (D) nickel-free or nickel-bound full-length NikR. For the nickel-bound form of the C-domain and full-length NikR in (C) and (D), the same distribution was observed when the absorbance was monitored at a nickel-dependent wavelength (302 nm) or a protein-dependent wavelength (276 nm). The lines are linear fits of the data and correspond to average molecular weights of 39.4 and 38.9 kDa for nickel-free and nickel-bound C-domain (expected tetramer Mr 37.5 kDa) and 62.6 and 54.3 kDa for nickel-free and nickel-bound full-length NikR (expected tetramer Mr 60.5 kDa).

same for the C-domain and NikR, the intensities of these peaks were not identical, suggesting some differences in the nickel binding sites of the full-length protein and the C-domain.

C-Domain and NikR Are Tetramers

Analytical ultracentrifugation was used to determine the oligomeric state of the purified C-domain and of full-length NikR, both as nickel-bound proteins and as nickel-free proteins (Figures 1C and 1D). In each case, the full-length protein or the C-domain behaved as a tetramer in sedimentation equilibrium experiments performed at protein concentrations of 20, 50, and 100 μM either in the presence or the absence of nickel. These results show that nickel binding is not required for protein tetramerization. Because the purified N-domain of NikR is dimeric [6], these results also demonstrate that the C-domain is responsible for the ability of NikR to form stable tetramers.

Nickel Affinity

Equilibrium data for the binding of nickel to the C-domain and intact NikR were obtained using titrations in which the free nickel concentration was buffered by EGTA. These experiments were performed with 50 μM protein, a concentration where both C-domain and full-length NikR are tetrameric. Figure 2 shows binding curves for the C-domain and full-length NikR. At saturation, in each case, the ratio of bound nickel to total protein subunits was found to be 1:1 (see Experimental Procedures). Both intact NikR and the isolated C-domain bound Ni^{2+} ions tightly, with half-maximal binding at free nickel concentrations of 2–7 pM (Table 1A). The best fits for the nickel binding isotherms were obtained using the Hill equation with coefficients of 1.4 to 2.2, indicative of positive cooperativity in nickel binding to the sites in NikR or its C-domain.

The isolated C-domain bound nickel about 3-fold more strongly than did intact NikR (Table 1A), suggesting that the N-domain in intact NikR interferes with metal binding to a small degree. Nickel binding to NikR was also 2- to 3-fold stronger in the presence of DNA fragments containing a full operator or an operator half-site (data not shown). Because Ni-EGTA at the concentrations used in these experiments inhibits NikR binding to DNA (data not shown), a quantitative assessment of the expected effect of nickel binding on DNA binding affinity was not possible based on these experiments. However, the data at least suggest that the interaction of the N-domain with operator DNA alters the nickel binding properties of the C-domain in intact NikR.

Preliminary kinetic experiments showed that the high-affinity nickel-bound states of NikR and the C-domain

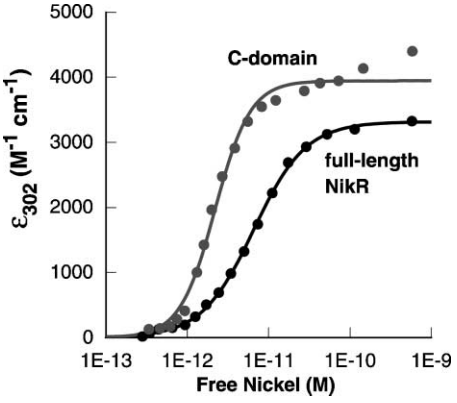

Figure 2. Nickel Affinity

Nickel titrations were performed in the presence of 1 mM EGTA, and the free nickel concentration for each data point was calculated from Equation 2.

Table 1. Nickel and NikR Operator Binding

A. Nickel Binding Properties[a]

Species	ϵ_{302} ($M^{-1}\cdot cm^{-1}$)	Half-Maximal Binding[b]	Hill Constant
Full-length NikR	3200	6.8×10^{-12} M	1.4
C-domain	3945	2.2×10^{-12} M	2.2

B. DNA Binding Properties

	50 μM nickel	
	Half-Maximal Binding[c]	Hill Constant
NikR (100 mM NaCl 20°C)	16×10^{-12} M	1.3
NikR (100 mM KCl, 20°C)	11×10^{-12} M	1.2
NikR (100 mM KCl, 37°C)	10×10^{-12} M	1.3
	1:1 nickel:NikR[d]	
NikR (100 mM NaCl 20°C)	33×10^{-9} M	1.6
NikR (100 mM KCl, 20°C)	54×10^{-9} M	1.1
NikR (100 mM KCl, 37°C)	39×10^{-9} M	1.2

[a] Determined from Figure 2.
[b] Average from two experiments.
[c] Average from three mobility shift experiments.
[d] Average from two footprinting experiments.

were stable for hours in the presence of metal binding competitors such as NTA and EDTA.

Nickel Effects on Protein Structure and Stability

The circular-dichroism (CD) spectrum of the nickel-free C-domain suggested a mixed α/β structure (Figure 3A). Addition of one nickel molecule per protein subunit increased the negative CD ellipticity both of the C-domain and of full-length NikR (Figure 3A). CD-difference spectra of the nickel-bound and nickel-free forms of the C-domain and of full-length NikR were essentially the same (Figure 3B), with a minimum near 218–220 nm and a maximum near 240 nm. The spectral change at 240 nm in the difference spectrum is likely to result from nickel-ligand interactions. The spectral change at 218–220 nm probably results from additional, nickel-induced secondary structure in the C-domain.

To test for potential conformational changes, we carried out sedimentation velocity experiments using the nickel-bound and nickel-free forms of full-length NikR. These studies showed that nickel-free NikR sedimented more rapidly than nickel-bound NikR (Figure 3C), suggesting that the nickel-free form was more compact.

At a concentration of 5 μM, nickel-free NikR unfolded cooperatively with two major denaturation transitions (Figure 4A). The second of these transitions, which mirrors unfolding of the isolated N-domain, occurred with a midpoint of roughly 6 M urea (Figure 4A). The first occurred at the same urea concentrations as unfolding of the isolated nickel-free C-domain (Figure 4B), which was relatively unstable with a midpoint of roughly 1 M urea. These results suggest that the N-domain and C-domain denature in relatively independent fashions in nickel-free NikR. Addition of 1:1 nickel to the C-domain resulted in biphasic denaturation (Figure 4B). At protein concentrations of 50 μM, the transition of the isolated C-domain shifted to a higher urea concentration, as did both transitions in intact NikR (data not shown). Addition of 1:1 nickel to intact NikR affected only the transition ascribed to the C-domain. This stability effect appeared to be specific, as addition of a stoichiometric quantity of cobalt to NikR produced the same CD spectral change seen in Figure 4A but had no effect on the denaturation profile of NikR (data not shown).

Nickel and Operator-DNA Binding

How does nickel binding to the C-domain of NikR affect binding to operator DNA? DNase I footprinting experiments were used to examine the effects of nickel on NikR binding to the *nik* operator in the P_{nik} promoter. No footprint was observed for nickel-free NikR at the highest protein concentration tested (≈1 μM). For nickel-bound NikR, the 40-bp footprint (Figure 5A) and corresponding binding curve (Figure 5B) showed half-maximal protection at a protein concentration of 30 nM with a Hill coefficient of 1.5. These results show that high-affinity nickel binding increased the apparent affinity of NikR for operator DNA by more than 30-fold. The Hill coefficient of 1.5 is consistent with the presence of some NikR dimers at the low concentrations used in these experiments, which subsequently bind operator DNA as tetramers.

High-affinity nickel binding is not sufficient for the highest-affinity NikR operator binding. In previous work, for example, we showed that NikR bound operator DNA with an apparent affinity near 15 pM at 20°C in the presence of 50 μM nickel [4]. This apparent affinity for operator DNA is roughly 1000-fold stronger than that observed here for the binding of nickel-bound NikR alone and indicates that a second, lower-affinity nickel site must influence operator binding. To test this model, we used footprinting to assay operator protection by 10 nM nickel-bound NikR as increasing amounts of excess nickel were added to the binding buffer. As shown in Figure 5C, only 5%–10% protection was observed using 10 nM nickel-bound NikR without excess nickel. As excess nickel was added, however, strong footprinting became evident (Figure 5D). Fitting of these data gave half-maximal occupancy of the low-affinity metal site at concentration of approximately 30 μM nickel with a Hill

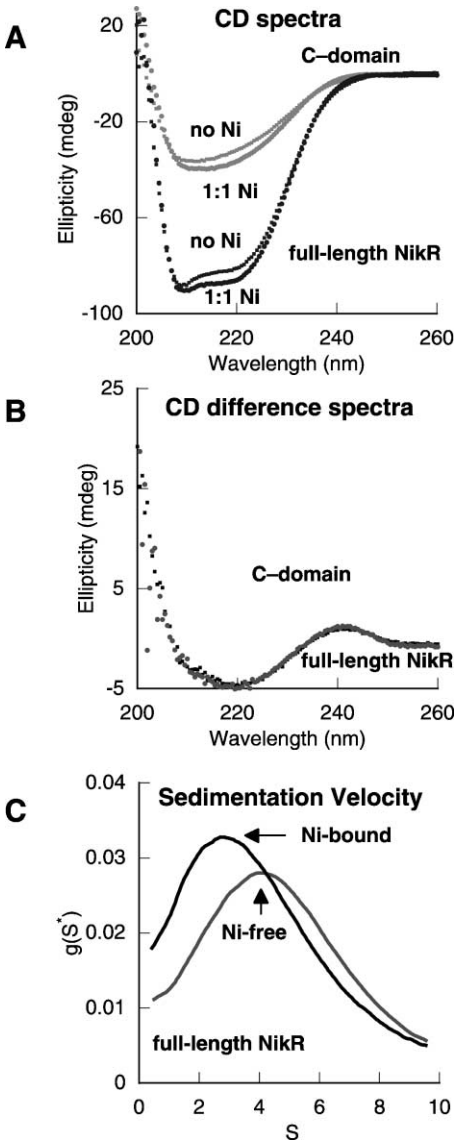

Figure 3. Effect of Nickel on Secondary Structure

(A) Far UV CD spectra of the C-domain and full-length NikR in the presence and absence of 1:1 nickel. Spectra were collected at 25°C in 20 mM Tris (pH 7.5).

(B) Difference spectrum of the nickel-free minus nickel-bound forms of the C-domain and full-length NikR.

(C) Average S value from sedimentation velocity experiments at 20°C with nickel-free and nickel-bound NikR at concentrations of 50 μM in 20 mM Tris (pH 7.5), 100 mM NaCl.

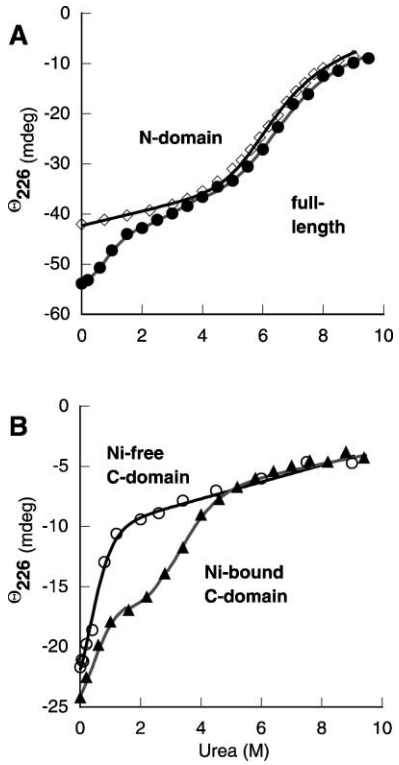

Figure 4. Stability to Urea Denaturation

Denaturation (A) nickel-free N-domain and nickel-free full-length NikR or (B) nickel-free C-domain and nickel-bound C-domain. Each sample was 5 μM in subunit equivalents. Data were collected at 20°C in 20 mM Tris (pH 7.5).

coefficient of 1.6. This Hill value indicates positive cooperativity and the participation of more than one low-affinity nickel ion in the very high-affinity complex of NikR with its operator. Temperature (20°C versus 37°C) or cations (KCl versus NaCl) had little effect on DNA binding by NikR either in the presence of 1:1 nickel or with 50 μM nickel (Table 1B).

When nickel concentrations were in excess of 20 μM, however, the NikR operator footprints revealed a much larger region of protection (cf. Figures 5A and 5B). Apparently, occupancy of the low-affinity Ni^{2+} binding sites in NikR allows an extensive set of new contacts with operator DNA. More than 30 base pairs on either side of the core *nik* operator were required before a stable gel shift could be observed (our unpublished results), suggesting that these new contacts are important for high-affinity DNA binding.

NikR Levels In Vivo

To determine intracellular NikR levels, *E. coli* strain MG1655 was grown anaerobically, and a small portion of the culture was used to determine the total cell number by serial dilutions and plating. Cells in the remaining portion of the culture were harvested, lysed, and NikR was purified by Ni-NTA affinity chromatography. Gel-shift assays of this partially purified material were compared to assays of purified NikR, allowing calculation of the concentration of the partially purified NikR. Cells grown at 37°C in LB broth without nickel or with 80 nM nickel both contained about 125 molecules of NikR. This number corresponds to an intracellular NikR concentration of roughly 200 nM based on a cell volume of 10^{-15} l. The actual value could be somewhat higher if losses of NikR occurred during purification. Nevertheless, 200 nM NikR with its high-affinity nickel sites filled should result in substantial occupancy of the *nik* operator, based on the binding curves shown in Figure 5. These

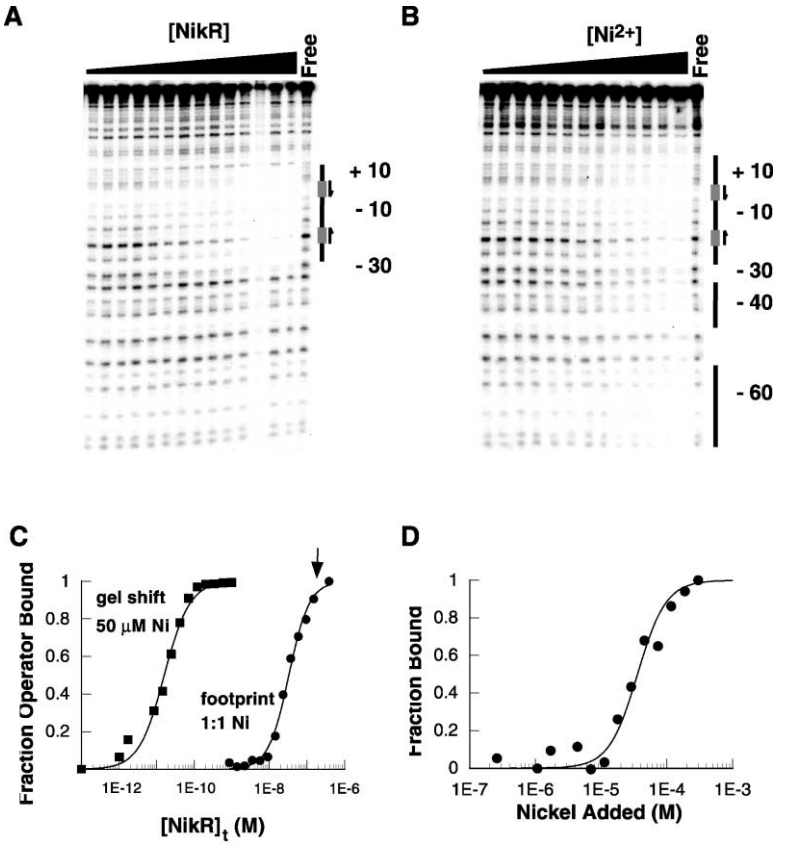

Figure 5. Nickel Dependence of DNA Binding

(A) Titration of 1:1 nickel-bound full-length NikR against a 120-bp operator DNA fragment from the *nikABCDE* promoter. The footprint is indicated by a black bar. Numbering corresponds to the start of the *nikABCDE* transcript. The gray bars and arrows represent the dyad-symmetric half-sites present in the *nik* promoter.

(B) Titration of nickel against 10 nM NikR and operator DNA. The extended footprint is indicated by black bars.

(C) DNA binding curve from the the experiment in (A) and a gel-shift assay performed in the presence of 50 μM nickel (data not shown). The arrow represents the approximate intracellular NikR concentration.

(D) Nickel binding curve from the experiment in (B). Footprinting experiments were performed in 20 mM Tris (pH 7.5), 100 mM KCl, 1 mM $MgCl_2$, 0.01% NP40, and 5% glycerol at 20°C with and without excess nickel. Gel-shift experiments were performed in the same buffer with 50 μM added nickel.

results indicate that nickel binding to the high-affinity NikR sites should result in a significant increase in operator binding in vivo.

Discussion

The experiments reported here demonstrate that the C-terminal domain of the *E. coli* NikR repressor mediates two molecular processes, nickel binding in the pM affinity regime and protein tetramerization. Based on the presence of conserved His, Cys, and Glu residues in the NikR family, it had been anticipated that the C-domain would bind nickel [4, 6]. The role of the C-domain in stabilizing NikR tetramerization was unexpected. Nickel binding is not required for tetramerization of either the C-domain or intact NikR. Previous work had shown that dimers of the N-terminal domain of NikR bound weakly but independently to each half of the *nik* operator, recog-

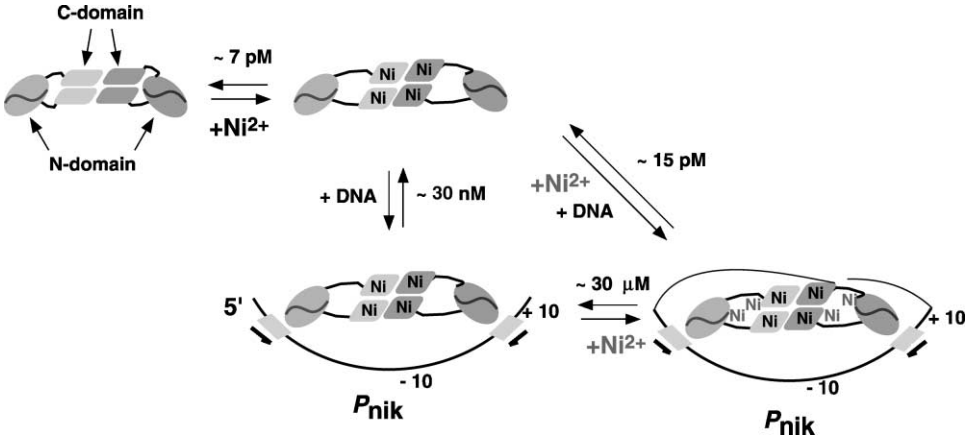

Figure 6. Free and DNA-Bound States of NikR

Apparent affinity constants for the ligand interactions are listed. Because of cooperativity, these affinity constants do not represent equilibrium constants.

nizing palindromic GTATGA sequences with a center-to-center separation of two turns of the DNA helix [4]. Higher affinity operator binding by NikR required the presence of both the C-terminal domain and high concentrations of nickel [4].

The C-terminal domain could affect the operator binding properties of NikR in two basic ways. First, this domain could link the DNA binding affinities of the two N-domain dimers in the tetramer, increasing their effective binding concentrations and the resulting affinity of NikR for operator. Second, nickel binding could mediate enhanced operator affinity either directly or through conformational changes in either domain. High-affinity nickel binding certainly represents a major function of the C-terminal domain in enhancing operator affinity. Additionally, the more extended structure of NikR upon nickel binding is consistent with some interaction between the N- and C-domains in the nickel-free form of the protein that could inhibit DNA binding by NikR. Tetramerization, in the absence of nickel binding, does not appear to play a dominant role in enhanced DNA binding. In fact, binding of nickel-free NikR tetramers to operator DNA was undetectable by footprinting ($K_d > 5$ μM) under the assay conditions used here. Additional studies will be required to determine the importance of C-domain tetramerization in increasing the affinity of nickel-bound NikR for operator DNA.

The experiments presented here confirm the previous suggestion of two distinct classes of nickel binding sites in NikR [4] and show that occupancy of these sites mediates radically different strengths and types of operator binding by NikR. Four high-affinity sites in the NikR tetramer are occupied by nickel with an apparent affinity of 7 pM. Interestingly, the coordination geometry of this high-affinity nickel site in NikR appears to be unique, based on X-ray absorption spectroscopy studies (F. Al-Mjeni, P.T.C., P.E. Carrington, R.T.S., and M.J. Maroney, submitted). Given an intracellular NikR concentration of 200 nM, introduction of a single free nickel molecule into a bacterial cell (1.6 nM) would result in greater than 99.99% binding of this ion to NikR at equilibrium and in the absence of competing nickel binding proteins. NikR is clearly capable of sensing extremely low concentrations of free nickel in the cell. The ZntR and Zur zinc-regulatory proteins of *E. coli* bind to their cognate metal ions with even stronger dissociation constants than NikR [9, 10]. Hence, the ability to sense single free metal ions in the cell may be a general property of metal-regulatory proteins. Binding of nickel to the high-affinity sites in NikR increases the apparent operator affinity from undetectable levels to roughly 30 nM and generates an operator footprint that covers about 40 base pairs of DNA. If all of the high-affinity nickel binding sites of NikR were occupied, an operator affinity of 30 nM would result in binding to the *nik* operator in roughly 90% of the cells. Substoichiometric binding of nickel to the high-affinity sites would clearly reduce the degree of operator binding.

The strongest binding of NikR to operator DNA (apparent affinity 10–15 pM) is observed in the presence of nickel concentrations that are more than 10^6-fold higher than those required to bind the high-affinity sites [4]. In footprinting assays, these low-affinity nickel binding sites of NikR were occupied with an apparent affinity of roughly 30 μM. Although nickel binding to this second set of sites is weak, it increases the affinity of NikR for the *nik* operator by roughly 1000-fold. A simple model of the linkage of nickel binding to both sets of sites and operator-DNA binding is shown schematically in Figure 6. At present, it is not known whether residues in the C-domain or the N-domain play roles in low-affinity nickel binding, or indeed, whether the low-affinity nickel sites exist in free NikR tetramers or are only present in NikR-operator complexes. Occupancy of both sets of nickel sites does, however, result in a near doubling of the number of operator bases protected from DNase I cleavage by bound NikR. Further studies will be required to determine whether these additional NikR-DNA contacts involve base-specific interactions.

It will also be important to determine whether both sets of nickel binding sites in NikR play roles in biological regulation. In principle, the use of both types of sites could allow NikR to sense intracellular nickel concentrations ranging from as low as one to as high as ten thousand molecules per cell and respond by altering *nikABCDE* expression appropriately. Disruption of NikR results in constitutive expression of the *nik* operon [5], but levels of *nikABCDE* transcription have not been measured as a function of nickel concentration. Occupancy of the high-affinity nickel sites may result in a NikR-operator complex that enhances *nik* gene expression in *E. coli*. Recently, the NikR ortholog from *Helicobacter pylori* was shown to activate expression of the urease genes in a nickel-dependent manner [11]. By this model, intracellular nickel concentrations beyond those required would result in occupancy of the low-affinity nickel sites and enable a change in the operator complex to a form that repressed *nikABCDE* expression and the import of additional nickel. This model is speculative but testable. One potential caveat may be the permissible concentrations of free intracellular nickel. For example, the intracellular levels of free transition metal ions, such as copper and zinc, in cells are believed to be essentially zero [9, 12]. Were this also the case for nickel, then occupancy of the low-affinity nickel sites in NikR might be biologically irrelevant or might only occur if other intracellular components stabilized this binding. In the former case, high-affinity nickel binding would be sufficient to repress *nikABCDE* transcription.

In addition to having homologous DNA binding domains, some ribbon-helix-helix family members share additional features with NikR. For example, P22 Mnt repressor is also tetrameric, but its C-terminal tetramerization domain forms a four-helix coiled-coil [13, 14]. The C-domain of NikR shows no sequence similarity to the C-domain of Mnt, and the circular-dichroism spectrum of the NikR C-domain is inconsistent with coiled-coil formation. MetJ and NikR are the only known ribbon-helix-helix proteins whose DNA binding is strongly enhanced by ligand binding. In the case of MetJ, binding of S-adenosyl methionine increases operator affinity by 25-fold [15], apparently through improved electrostatics with the DNA [16]. Nickel binding to NikR might also affect the electrostatics of operator binding, but determination of the structure of NikR in its different nickel-bound and DNA-bound forms will be required to assess this possibility rigorously.

Significance

The regulation of trace-metal concentration is a problem for all organisms because a balance must be achieved between too little and too much metal. Appropriate genetic and physiological responses are required in both cases to ensure the survival and optimal growth of the organism. In this study, we have shown that NikR, a conserved transcriptional regulator, is capable of sensing nickel at concentrations corresponding to a range from 1 to 10,000 molecules per cell. Strong (pM) and weak (μM) binding sites are used to sense nickel at each end of this range. Occupancy of the strong nickel sites activates binding NikR tetramers to operator DNA with an affinity (30 nM) that should ensure substantial operator binding in the cell. Binding to the weak nickel sites leads to an additional 1000-fold increase in operator affinity and a substantial change in the conformation of the protein-DNA complex. The existence of two nickel-dependent NikR operator complexes raises the possibility that these complexes affect transcription of the *nikABCDE* operon in distinct fashions.

Experimental Procedures

Cloning and Mutagenesis

A gene encoding the NikR C-fragment (residues 48–133) was created by PCR amplification from pNIK103 [4]. The resulting fragment was digested with NdeI/XhoI and ligated into pET-22b (Novagen, Madison, WI) digested with the same enzymes. The nucleotide sequence of the NikR C-domain (pNIK102) was confirmed by DNA-sequencing (MGH Sequencing Facility).

Protein Purification

The NikR C-domain or full-length NikR were expressed in *E. coli* strain DL41 (Coli Genetic Stock Center), nickel was added to the lysate, and the proteins were purified by Ni-NTA agarose affinity chromatography as described [4]. After elution from the Ni-NTA column, the eluant was diluted 4-fold with deionized H_2O and applied to a 1 × 5 cm column of Q-Sepharose (Pharmacia) equilibrated with 20 mM Tris (pH 8.3), 100 mM NaCl. After the sample was loaded, the column was washed with 2 volumes of equilibration buffer, and protein was eluted with a 100 ml gradient from 100 mM to 1 M NaCl. All steps were performed at 20°C. Fractions containing the C-domain or NikR mutants were identified by SDS-PAGE, pooled, concentrated using a Millipore Ultrafree-4 filter unit, and stored at 4°C. Protein concentrations in monomer equivalents were determined in 6 M GuHCl using extinction coefficients (276 nm) of 4440 $M^{-1}cm^{-1}$ for NikR and 2960 $M^{-1}cm^{-1}$ for the purified C-domain.

Generation of Nickel-free Proteins

Purified C-domain or NikR was incubated with 50 mM EDTA (0.5 M stock [pH 8.0]) in 20 mM Tris (pH 8.3), 1 M NaCl for 48 hr at 4°C. At this time, the UV-visible spectra showed no evidence of residual bound nickel. Prior to characterization, the nickel-free proteins were desalted into an appropriate buffer using a P6 spin column (Biorad).

UV-Visible Spectroscopy and Nickel Titrations

UV-visible spectroscopy was performed using a Hewlett-Packard 8452A diode array spectrophotometer. Titration experiments used a range of nickel concentrations in 10 mM HEPES (pH 7.5), 100 mM NaCl, and 1 mM EGTA at 20°C [17, 18]. Nickel-free protein was desalted into titration buffer and was added to separate tubes containing increasing amounts of total nickel. Samples were incubated at 20°C for at least 30 min. No difference was observed in the absorbance of samples incubated for times up to 4 hr. The fraction of nickel bound was determined by the absorbance at 302 nm and Equation 1:

$$\nu = A_i/A_{max}. \quad (1)$$

The concentration of free nickel present for each total nickel concentration was calculated from Equation 2:

$$(1/K_{Ni})[Ni]_f^2 + \{(1/K_{Ni})\{[EGTA]_t - [Ni]_t + \nu[NikR]_t\} + 1\}[Ni]_f + \nu[NikR]_t - [Ni]_t = 0 \quad (2)$$

where $[EGTA]_t$, $[Ni]_t$, and $[NikR]_t$ are the total concentrations of EGTA, Ni, and NikR, respectively. K_{Ni} is the equilibrium dissociation constant (3.16×10^{-14} M) of EGTA for Ni at pH 7.5, I = 0.1 M [19]. The free nickel concentration was plotted against ν, and the equilibrium dissociation constant of NikR or the C-domain for nickel was determined using Equation 3, a form of the Hill equation:

$$\nu = 1/\{1+(K_{app}/[Ni]_f)^n\}. \quad (3)$$

To determine stoichiometries, samples at the titration endpoints were desalted to remove Ni-EGTA, and nickel bound to the protein was assayed using PAR, a divalent metal indicator [20].

Circular Dichroism and Chemical Stability

Circular-dichroism (CD) spectra were taken using an AVIV 60DS spectrapolarimeter as described [6]. The sample buffer was 20 mM Tris (pH 7.5). For measurements of the nickel-bound forms of NikR or C-domain, nickel was added in a 1:1 molar ratio to the nickel-free protein. Urea denaturation curves were determined using separate samples for each urea concentration. Samples were incubated for at least 6 hr at 20°C. CD ellipticity was measured at 226 nm.

Analytical Ultracentrifugation

Equilibrium centrifugation experiments in a Beckman XL-A instrument were carried out at 20°C as described [6] in 20 mM Tris (pH 7.5), 100 mM NaCl. For measurements of the nickel-bound forms of NikR or C-domain, nickel was added in a 1:1 molar ratio to the nickel-free protein. Data were collected at three different speeds (8,000, 13,000, and 24,000 rpm). Partial molar volumes were calculated using the program SEDNTERP 1.0 (http://www.jphilo.mailway.com) and were assumed to be the same for the nickel-free and nickel-bound forms of NikR or the C-domain. Data were fit to Equation 4:

$$M_w = m^*2RT/\{(1-\nu\rho)\omega^2\}. \quad (4)$$

Sedimentation velocity experiments were carried at 20°C in 20 mM Tris (pH 7.5), 100 mM NaCl. Scans were taken every 2 min for 4 hr at a rotor speed of 40,000 rpm. Nickel-bound full-length NikR and nickel-free full-length NikR sedimentation were monitored at 300 and 276 nm, respectively. Data were fit using the velocity fitting feature of the Beckman XL-A software.

DNA Binding Assays

DNase I footprinting and gel mobility shifts assays were performed as described [4]. The DNA fragment was generated by PCR amplification of a 500-bp fragment from pPC163 [4] followed by digestion with ClaI. The smaller 120-bp fragment was isolated and labeled by end filling using α^{32}P-dCTP and Sequenase (USB, Cleveland, OH). Attempts to carry out EGTA-buffered nickel titrations in the presence of DNA were hampered by the apparent formation of a Ni-EGTA:DNA complex that inhibited NikR binding (data not shown). Footprinting reactions were carried out at 20°C or 37°C. Gel shifts were performed as described [4]. Binding reactions were equilibrated at either 20°C or 37°C. Footprint and gel-shift binding data were fit to the Hill equation to determine an apparent binding constant and Hill coefficient.

Determination of Intracellular NikR Levels

E. coli strain MG1655 was inoculated in LB media filled to the top of 1 liter sealed centrifuge bottles (approximately 1040 ml). The cultures were grown without shaking for 20 hr at 37°C. A small aliquot (<200 μl) of culture was removed to determine the optical density as well as the number of viable cells present. The OD_{600} measurements ranged from 0.59 to 0.62. To determine number of viable cells, dilutions of up to 10^8-fold were plated on solid LB agar

and grown at 37°C for 12 hr. The 10^7-fold dilutions of different bottles had 225–250 viable cells/ml, corresponding to 2.3 to 2.6 $\times$ 10^{12} total cells. Partial purification of the cell lysate was carried out using the Ni-NTA procedure described above. NikR activity in each sample was determined by gel-shift assay [4].

Acknowledgments

We thank David Wah and Randy Burton for assistance with ultracentrifugation experiments, members of the Sauer lab for helpful discussions, and Mike Maroney for comments on the manuscript. This work was supported by a Merck/MIT Postdoctoral Fellowship (P.T.C.) and NIH grants AI-16897 and AI-15706.

Received: August 2, 2002
Revised: September 5, 2002
Accepted: September 11, 2002

References

1. Hausinger, R.P. (1987). Nickel utilization by microorganisms. Microbiol. Rev. *51*, 22–42.
2. Maroney, M.J. (1999). Structure/function relationships in nickel metallobiochemistry. Curr. Opin. Chem. Biol. *3*, 188–199.
3. Ballantine, S.P., and Boxer, D.H. (1985). Nickel-containing hydrogenase isoenzymes from anaerobically grown *Escherichia coli* K-12. J. Bacteriol. *163*, 454–459.
4. Chivers, P.T., and Sauer, R.T. (2000). Regulation of high-affinity nickel uptake in bacteria: Ni^{2+}-dependent interaction of NikR with wild-type and mutant operator sites. J. Biol. Chem. *275*, 19735–19741.
5. de Pina, K., Desjardin, V., Mandrand-Berthelot, M.-A., Giordano, G., and Wu, L.-F. (1999). Isolation and characterization of the *nikR* gene encoding a nickel-responsive regulator in *Escherichia coli*. J. Bacteriol. *181*, 670–674.
6. Chivers, P.T., and Sauer, R.T. (1999). NikR is a ribbon-helix-helix DNA-binding protein. Protein Sci. *8*, 2494–2500.
7. Phillips, S.E. (1994). The beta-ribbon DNA recognition motif. Annu. Rev. Biophys. Biomol. Struct. *23*, 671–701.
8. Raumann, B.E., Brown, B.M., and Sauer, R.T. (1994). Major groove DNA recognition by β-sheets: the ribbon-helix-helix family of gene regulatory proteins. Curr. Opin. Struct. Biol. *4*, 36–43.
9. Outten, C.E., and O'Halloran, T.V. (2001). Femtomolar sensitivity of metalloregulatory proteins controlling zinc homeostasis. Science *292*, 2488–2492.
10. Hitomi, Y., Outten, C.E., and O'Halloran, T.V. (2001). Extreme zinc-binding thermodynamics of the metal sensor/regulator protein, ZntR. J. Am. Chem. Soc. *123*, 8614–8615.
11. van Vliet, A.H.M., Poppelars, S.W., Davies, B.J., Stoof, J., Bereswill, S., Kist, M., Penn, C.W., Kuipers, E.J., and Kusters, J.G. (2002). NikR mediates nickel-responsive transcriptional induction of urea expression in *Helicobacter pylori*. Infect. Immun. *70*, 2846–2852.
12. Rae, T.D., Schmidt, P.J., Rufahl, R.A., Culotta, V.C., and O'Halloran, T.V. (1999). Undetectable intracellular free copper: the requirement of a copper chaperone for superoxide dismutase. Science *284*, 748–749.
13. Waldburger, C.D., and Sauer, R.T. (1995). Domains of the Mnt repressor: roles in tetramer formation, protein stability, and operator DNA binding. Biochemistry *34*, 13109–13116.
14. Nooren, I.M., Kaptein, R., Sauer, R.T., and Boelens, R. (1999). The tetramerization domain of the Mnt repressor consists of two right-handed coiled coils. Nat. Struct. Biol. *6*, 755–759.
15. Hyre, D.E., and Spicer, L.D. (1995). Thermodynamic evaluation of binding interactions in the methionine repressor system of *Escherichia coli* using isothermal titration calorimetry. Biochemistry *34*, 3212–3221.
16. Phillips, K., and Phillips, S.E.V. (1994). Electrostatic activation of *Escherichia coli* methionine repressor. Structure *2*, 309–316.
17. Mely, Y., Cornille, F., Fournie-Zaluski, M.C., Darlix, J.L., Roques, B.P., and Gerard, D. (1991). Investigation of zinc-binding affinities of Moloney murine leukemia virus nucleocapsid protein and its related zinc finger and modified peptides. Biopolymers *31*, 899–906.
18. Guo, J., and Giedroc, D.P. (1997). Zinc site redesign in T4 gene 32 protein: structure and stability of cobalt(II) complexes formed by wild-type and metal-ligand substitution mutants. Biochemistry *36*, 730–742.
19. Martell, A.E., and Smith, R.M. (1989). Critical Stability Constants. (New York: Plenum Press).
20. Hunt, J., Neece, S., and Ginsburg, A. (1985). The use of 4-(2-pyridylazo)resorcinol in studies of zinc release from *Escherichia coli* aspartate transcarbamoylase. Anal. Biochem. *146*, 150–157.